2024 IEEE International Conference on Robotics and Automation (ICRA 2024)
May 13-17, 2024. Yokohama, Japan

Investigation on the multi-solution problem of the kinetostatics of cable-driven continuum manipulators

Yicheng Dai [1,2], Zuan Li [3], Xin Wang [1], Han Yuan [1,2,*], *Member, IEEE*

Abstract—Cable-driven continuum manipulators have gained considerable attention due to their high dexterity and inherent structural compliance, making them a popular research topic. However, previous studies have overlooked the kinetostatics of these manipulators, which can result in a multi-solution problem. This issue is critical as having multiple equilibrium states can lead to erroneous estimations of the manipulator's profile. To address this issue, the kinetostatic model is presented and simulations based on both the interval analysis method and the commonly used floating-point optimization algorithm are conducted under the same actuating forces and external loads. Results show that there are multiple solutions to the kinetostatics of cable-driven continuum manipulators with constant cross section or variable cross section. This paper fills a gap in the current literature and offers valuable insights for researchers in the field of cable-driven continuum manipulators.

Keywords: Cable-driven continuum manipulator; Kinetostatics; Multi-solution problem; Interval analysis.

I. INTRODUCTION

Continuum manipulators are a product of the deep integration between bionics and robotics. The structure of continuum manipulators is the imitation of the continuous flexible structures found in nature, such as the elephant's trunk [1], or the octopus's tentacles [2]. These manipulators utilize the deformation of elastic bodies to cause bending and movement of their structures, resulting in an infinite number of degrees of freedom. Their slender body enables them to easily maneuver and operate in confined spaces, such as equipment monitoring and maintenance [3], post-disaster rubble exploration and rescue [4], or minimally invasive surgery [5]. Furthermore, the mechanical-electrical separation of continuum manipulators allows them to operate effectively in harsh environments, such as space [6] or nuclear power plants [7].

Their structure typically consists of a highly elastic central backbone as support, with a certain number of spacers distributed on the central backbone. Variable prototypes have been presented. For instance, Dong proposed a cable-driven continuum manipulator for engine inspection [8]. Yang [9] presented a prototype which uses shape memory alloys as a trigger to realize variable stiffness. In [10], a kind of continuum manipulator with the twin-pivot compliant mechanism is proposed.

* This work was supported by the National Natural Science Foundation of China (Grants No. 62173114), the Science and Technology Innovation Committee of Shenzhen (Grants No. JCYJ20210324115812034, JCYJ20210324115811033,), and the Program of Shenzhen Peacock Innovation Team (Grant No. KQTD20210811090146075). (Corresponding author: Han Yuan).

Y. Dai, X. Wang and H. Yuan are with the School of Mechanical Engineering and Automation, Harbin Institute of Technology (Shenzhen), Shenzhen 518055, China. Y. Dai and H. Yuan are also with the Guangdong Provincial Key Laboratory of Intelligent Morphing Mechanisms and Adaptive Robots, and Key University Laboratory of Space Mechanisms and Robots of Guangdong, 518055 Shenzhen, China. Z. Li is with the Aerospace Research and Development Center, Shanghai Aerospace Control Technology Institute, Shanghai 201109, China. (e-mail: daiyicheng94@gmial.com; lee347572930@163.com; wangxinsz@hit.edu.cn; yuanhan@hit.edu.cn).

To control a robot to perform desired operations, kinematic modeling is an important aspect. Unlike conventional robots with rigid joints and links, the bending deformation of cable-driven continuum manipulators is not only related to their own kinematic parameters but also to the manipulator's force state, making it a coupled problem of kinematics and statics. To obtain the profile of the manipulator, it is necessary to solve the kinematic and static equations of the manipulator simultaneously [11]. Currently, the most commonly used method for establishing a kinetostatic model for cable-driven continuum manipulators is the Newton-Euler recursive method [12].

However, most of the previous research has ignored the multi-solution problem of the kinetostatics of continuum manipulators. Mathematically, a nonlinear system consisting of kinematic and static equilibrium equations may have multiple solutions. Usually, the floating-point optimization algorithms are used to solve this nonlinear equation system [13]. However, this method can only find one solution, which has led to the neglect of the fundamental problem that there are multiple solutions for the kinetostatics of continuum manipulators. This issue is critical for continuum manipulators for several reasons. Firstly, the presence of multiple solutions means that the manipulator's profile is not unique. Secondly, when several adjacent equilibrium states are in close proximity, small external disturbances can cause the manipulator to suddenly transition from one equilibrium state to another, posing significant challenges for controlling the manipulator. Therefore, it is essential to identify all solutions to the kinetostatic problem.

This paper proposes a hypothesis that the kinetostatic problem of cable-driven continuum manipulators may have multiple solutions, meaning that the profile of the manipulator is not unique when the driving forces and loads are determined. Then, taking a planar cable-driven continuum manipulator with single section as an example, this paper proposes using interval analysis method to solve this problem and obtain all solutions in a specified workspace. Interval analysis was first proposed by R.E. Moore [14]. It is a numerical technique that allows all real solutions of a system of equations and/or inequalities to be obtained in a predetermined search domain [15]. The method based on interval analysis has been proven to be highly effective in solving the direct kinematics of rigid parallel robots [16]. In this paper, simulations based on interval analysis and the commonly used floating-point optimization algorithms are carried out to verify the proposed hypothesis. Then the results are compared and analyzed.

The rest of this paper is organized as follows. Section 2 presents the kinetostatic model of the continuum manipulators. In section 3, the interval analysis method and its calculation process are presented. Then simulation verifications and comparisons on continuum manipulators with constant cross section and variable cross section is carried out in Section 4. Finally, conclusions are made in Section 5.

II. Modeling

At present, there are many studies using the Newton-Euler method to establish the kinetostatic model of cable-driven continuum manipulators [17], [18]. In this section, a brief kinetostatic model is recalled, and more details can refer to our previous research [12]. In the process of establishing the kinetostatic models, the following assumptions are made:

(1) The elastic deformation of the central backbone between adjacent spacers is approximated as circular arcs with different curvatures;

(2) The deformation of the spacers and dimensional errors are not considered;

(3) The central backbone and spacers are made of homogeneous materials;

(4) The gravitational effect of spacers and central backbone is considered while the gravity force of the driving cables and the frictional effect is ignored.

A. Kinematic model

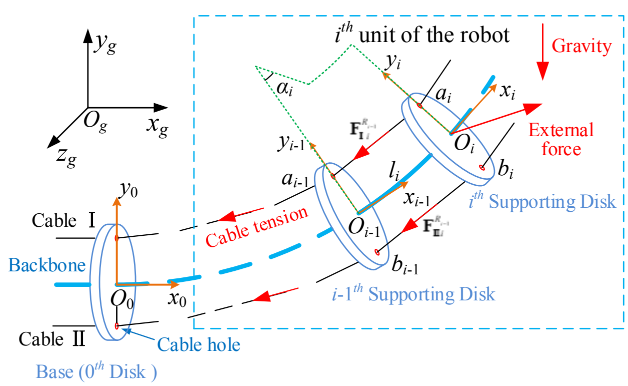

Fig. 1 Schematic of the section of a cable-driven continuum manipulator

This section recalls the method of establishing the kinematic model of the cable-driven continuum manipulator using homogeneous coordinate transformations [12]. The schematic of the manipulator's structure is shown in Figure 1. Note ${}^{R_{i-1}}\mathbf{T}_{R_i}$ as the homogeneous transformation matrix from the $(i-1)^{\text{th}}$ coordinate $R_{O_{i-1}}$ to the i^{th} coordinate R_{O_i}. Then the transformation matrix from the global coordinate R_{O_g} to any locale coordinate R_{O_m} $(0 < m \le n)$ can be written as:

$$ {}^{R_g}\mathbf{T}_{R_m} = {}^{R_g}\mathbf{T}_{R_0}\,{}^{R_0}\mathbf{T}_{R_m} = {}^{R_g}\mathbf{T}_{R_0}\prod_{i=1}^{m}{}^{R_{i-1}}\mathbf{T}_{R_i} \tag{1} $$

where ${}^{R_g}\mathbf{T}_{R_0}$ is the transformation matrix from R_{O_g} to the base coordinate R_{O_0}.

B. Static model

In this part, the Newton-Euler method is used to establish the static model of cable-driven continuum manipulators. Under the effect of the external load on the distal end, cable tension and the gravitational effect, the system keeps balance, as shown in Fig. 1.

Gravity force and torque

In this part, gravities of disks and central backbone on the continuum manipulator will be considered in kinetostatic modeling. For the i^{th} segment, the weight of the central backbone and the spacer are $\mathbf{g}_{si}^{R_g}$ and $\mathbf{g}_{di}^{R_g}$, respectively. Their expressions in the local coordinate system $R_{O_{i-1}}$ can be written as:

$$ \mathbf{g}_{di}^{R_{i-1}} = {}^{R_{i-1}}\mathbf{T}_{R_g}\mathbf{g}_{di}^{R_g} \tag{2} $$

$$ \mathbf{g}_{si}^{R_{i-1}} = {}^{R_{i-1}}\mathbf{T}_{R_g}\mathbf{g}_{si}^{R_g} \tag{3} $$

The relative gravitational moments can be expressed as:

$$ \mathbf{m}_{di} = \overrightarrow{O_{i-1}O_i}^{R_{i-1}} \times \mathbf{g}_{di}^{R_{i-1}} \tag{4} $$

$$ \mathbf{m}_{si} = \overrightarrow{O_{i-1}O_{G_{si}}}^{R_{i-1}} \times \mathbf{g}_{si}^{R_{i-1}} \tag{5} $$

where $O_{G_{si}}$ is the centroid of the central backbone.

External forces and moments

When there is interaction between the manipulator and the environment, in the global coordinate R_g, external forces and external moments are generated at the contact point, noted as $\mathbf{f}_{Ei}^{R_g}$ and $\mathbf{m}_{EFi}^{R_g}$. In the $R_{O_{i-1}}$ coordinate system, they can be written as:

$$ \mathbf{f}_{Ei}^{R_{i-1}} = {}^{R_{i-1}}\mathbf{T}_{R_g}\mathbf{f}_{Ei}^{R_g} \tag{6} $$

$$ \mathbf{m}_{EFi}^{R_{i-1}} = {}^{R_{i-1}}\mathbf{T}_{R_g}\mathbf{m}_{EFi}^{R_g} \tag{7} $$

In the $R_{O_{i-1}}$ coordinate system, the moments caused by $\mathbf{f}_{Ei}^{R_{i-1}}$ can be written as:

$$ \mathbf{m}_{Ei} = \overrightarrow{O_{i-1}O_i}^{R_{i-1}} \times \mathbf{f}_{Ei}^{R_{i-1}} \tag{8} $$

Actuating forces

As illustrated in Fig. 1, the driving force of cable 1 in coordinate $R_{O_{i-1}}$ is noted as $\mathbf{f}_{\mathrm{I}\,i}^{R_{i-1}}$. The tension along the direction of the cable can be written as:

$$ \mathbf{f}_{\mathrm{I}\,i}^{R_{i-1}} = \mathbf{f}_{\mathrm{I}\,i} + \mathbf{f}_{\mathrm{I}(i+1)} = \left|\mathbf{f}_{\mathrm{I}\,i}\right| \frac{\overrightarrow{a_i a_{i-1}}^{R_{i-1}}}{\left|\overrightarrow{a_i a_{i-1}}^{R_{i-1}}\right|} + \left|\mathbf{f}_{\mathrm{I}(i+1)}\right| \frac{\overrightarrow{a_i a_{i+1}}^{R_{i-1}}}{\left|\overrightarrow{a_i a_{i+1}}^{R_{i-1}}\right|} \tag{9} $$

Specially, when i=n, the driving force on the spacer can be written as:

$$\mathbf{f}_{\mathrm{I}\,n}^{R_{n-1}} = \left|\mathbf{f}_{\mathrm{I}\,n}\right| \frac{\overrightarrow{a_n a_{n-1}}^{R_{n-1}}}{|\overrightarrow{a_n a_{n-1}}^{R_{n-1}}|} \tag{10}$$

Then the concentrated moment on the origin of the coordinate $R_{O_{i-1}}$ can be expressed as:

$$\mathbf{m}_{\mathrm{I}\,i} = \overrightarrow{O_{i-1}a_i}^{R_{i-1}} \times \mathbf{f}_{\mathrm{I}\,i}^{R_{i-1}} \tag{11}$$

In the same way, the driving force and moments generated by cable 2 can be obtained by substituting a_i for b_i.

Kinetostatic equilibrium

In this part, the Newton-Euler method will be used to derive the equilibrium of the manipulator. As for the end segment:

$$\mathbf{f}_{n-1}^{R_{n-1}} = \mathbf{f}_{\mathrm{I}\,n}^{R_{n-1}} + \mathbf{f}_{\mathrm{II}\,n}^{R_{n-1}} + \mathbf{g}_{dn}^{R_{n-1}} + \mathbf{g}_{sn}^{R_{n-1}} + \mathbf{f}_{En}^{R_{n-1}} \tag{12}$$

$$\mathbf{m}_{n-1} = \mathbf{m}_{\mathrm{I}\,n} + \mathbf{m}_{\mathrm{II}\,n} + \mathbf{m}_{dn} + \mathbf{m}_{sn} + \mathbf{m}_{En}^{R_{i-1}} + \mathbf{m}_{EFn} \tag{13}$$

where $\mathbf{f}_{En}^{R_{n-1}}$ is the expression of external forces. $\mathbf{g}_{dn}^{R_{n-1}}$ and $\mathbf{g}_{sn}^{R_{n-1}}$ are the weight of the spacer and central backbone. They are all expressed in the $R_{O_{i-1}}$ coordinate system.

As for the i^{th} segment, the influence of the $(i+1)^{\mathrm{th}}$ (i=1, 2, …, n-1) segment can be expressed as:

$$\mathbf{f}_{i-1}^{R_{i-1}} = \mathbf{f}_{\mathrm{I}\,i}^{R_{i-1}} + \mathbf{f}_{\mathrm{II}\,i}^{R_{i-1}} + \mathbf{g}_{di}^{R_{i-1}} + \mathbf{g}_{si}^{R_{i-1}} + \mathbf{f}_{Ei}^{R_{i-1}} + \mathbf{f}_{i}^{R_{i-1}} \tag{14}$$

$$\mathbf{m}_{i-1} = \mathbf{m}_{ai} + \mathbf{m}_{bi} + \mathbf{m}_{di} + \mathbf{m}_{si} + \mathbf{m}_{Ei}^{R_{i-1}} + \mathbf{m}_{EFi} + \mathbf{m}_{i} + \mathbf{m}_{Fi} \tag{15}$$

where $\mathbf{f}_{i}^{R_{i-1}}$ and $\mathbf{m}_i$ are the force and torque generated by the $(i-1)^{\mathrm{th}}$ segment. $\mathbf{m}_{Fi}$ is the torque generated by $\mathbf{f}_{i}^{R_{i-1}}$ with respect to the origin O_{i-1}.

Based on the Euler-Bernoulli beam theory, the deflection angle of the i^{th} segment can be obtained:

$$\alpha_i = \frac{M_i}{E_i I_i} s_i \tag{16}$$

where E_i, I_i and s_i are the young's modulus, moment of inertia, and the length of the i^{th} segment, respectively.

Thus, the kinetostatic model of the continuum manipulator can be described by these equations, where gravitational forces, external loads, cable tensions and the rotation angle of each segment are coupled.

III. Solution by Interval Analysis Method

The kinetostatic model established in section 2 based on the Newton-Euler recursive method is a non-linear system of equations, for which analytical solutions are generally not feasible. Instead, numerical solutions can be obtained through floating-point optimization algorithms. However, this kind of point iteration method may not be able to find all solutions, whereas interval analysis method can realize it within a preset working space.

Compared to the floating-point iterative optimization algorithms, the interval analysis method offers several advantages for solving kinetostatic problems. First, the interval analysis method requires solutions to be obtained within a pre-determined interval, which can be defined as the working space of the continuum manipulator. This allows for the exclusion of solutions that do not align with the actual physical situation. Additionally, the interval analysis method ensures that results are free from the adverse effects of computer rounding errors, which is the original source and application direction of this method. The computational results of the interval analysis method remain as intervals, with the precise solution being strictly contained within the range. This allows for a direct reflection of the accuracy of the computed results based on the width of the obtained interval. Due to these advantages, we prioritize the use of interval analysis to solve the problem.

A. Introduction to interval analysis

This section provides a brief introduction to the fundamental concepts and important properties of interval algorithms. More detailed information can be found in literature [19]. Interval analysis was initially used to avoid the accumulation of errors caused by computer rounding. It has been used as a useful tool for handling uncertainties by replacing floating-point values with intervals as variables [19]. For instance, S. Iqbal developed an interval analysis based method to present the resolution of their proposed analytical inverse kinematics of continuum robots [20]. F. Hisch presented a robust tracking control approach using interval analysis [21]. However, none of these studies used this method to address the multi-solution problem of continuum robots.

There are multiple methods to realize interval evaluation of a function. A commonly used one is natural evaluation [22] , which means replacing the basic arithmetic operations and arithmetic functions of point arithmetic with equivalent interval forms. Generally, overestimation will be caused while carrying out interval evaluation through natural evaluation. Fortunately, this solution interval includes the real interval, ensuring the reliability of the solution. However, the influence on the calculation can be large if the overestimation is severe. Therefore, it is important to avoid severe overestimation. To avoid this, in this paper, the width of the interval is reduced by dividing the initial predefined space into multiple sub-intervals through repeated bisection and checking whether each sub-interval contains a solution.

Besides, inclusion of monotonicity is another important property of interval analysis. For example, if $\forall \boldsymbol{A}, \boldsymbol{B} \in \mathbf{R}$, $\boldsymbol{A} \subseteq \boldsymbol{B}$, then $\mathbf{F}(\boldsymbol{A}) \subseteq \mathbf{F}(\boldsymbol{B})$. Then it can be found that if $0 \notin \mathbf{F}(\boldsymbol{X})$, there is no solution in interval $\boldsymbol{X}$ to meet the requirement of $f(x)=0$. This is the criteria to determine if there is a solution in the interval. Usually, we will delete the interval without solution. In addition to this fast criterion, we need to use the Krawczyk-Hansen operator [23] to check the existence and uniqueness of the solutions within the sub-intervals. The Krawczyk-Hansen operator can be written as:

$$\mathbf{H}(\boldsymbol{X}) = y - \boldsymbol{Y} f(y) + \boldsymbol{L}(\boldsymbol{X})(\boldsymbol{H}'(\boldsymbol{X}) - y) + \boldsymbol{U}(\boldsymbol{X})(\boldsymbol{X} - y) \tag{17}$$

where $\forall y \in \boldsymbol{X}$, $\boldsymbol{Y}$ is an arbitrary nonsingular matrix. $\mathbf{H}'(\boldsymbol{X}) = \mathbf{H}(\boldsymbol{X}) \cap \boldsymbol{X}$. $\boldsymbol{L}(\boldsymbol{X})$ and $\boldsymbol{U}(\boldsymbol{X})$ are the lower and upper triangular interval matrix of $\left[\boldsymbol{I}-\boldsymbol{Y}\mathbf{F}'(\boldsymbol{X})\right]$. $\boldsymbol{I}$ is an identity matrix and $\mathbf{F}'(\boldsymbol{X})$ is the interval evaluation of the containing monotonicity of $f'(x)$ over interval $\boldsymbol{X}$.

It is convenient to determine the existence of solutions in the sub-interval using Krawczyk-Hansen operator.

(1) If $\mathbf{H}'(\boldsymbol{X})=0$, there is no solution in sub-interval $\boldsymbol{X}$;

(2) If $\mathbf{H}(\boldsymbol{X}) \subseteq \boldsymbol{X}$, there is solution in sub-interval $\boldsymbol{X}$ and the solution is in $\mathbf{H}'(\boldsymbol{X})$;

(3) If $\mathbf{H}(\boldsymbol{X}) \neq \varnothing$, sub-interval $\boldsymbol{X} \in \boldsymbol{D}$, $\boldsymbol{D} \subseteq \mathbf{R}^n$, $\mathbf{H}(y, \boldsymbol{X}) \subseteq \boldsymbol{X}$, $w(\boldsymbol{H}) < w(\boldsymbol{X})$, then there is a unique solution in sub-interval $\boldsymbol{X}$ and it is in $\mathbf{H}'(\boldsymbol{X})$.

According to the results of the Krawczyk-Hansen operator, we can determine whether a sub-interval should be kept or deleted. After multiple iterations of partitioning, when the size of the remaining sub-intervals meet the set accuracy requirements, they can be output as the complete solution set of the nonlinear equations.

B. Solving problem using interval analysis

The application of interval analysis to solve nonlinear equations can be summarized as an iterative process of subdivision, testing, and deletion, as shown in Fig. 2. These output sub-intervals can be used as solutions to the nonlinear equation system. Due to large scope of the initial interval, the computational time of the interval analysis algorithm is much higher than that of traditional floating-point optimization algorithms. Therefore, using mature and efficient software tools is necessary. There are many software tools available for running interval analysis algorithms on floating-point computers. These tools have undergone rigorous testing by their developers and any result is proven to be true under any circumstances. One of the most functionally complete and user-friendly interval analysis tools is INTLAB, which will be used to carry out simulations in this paper.

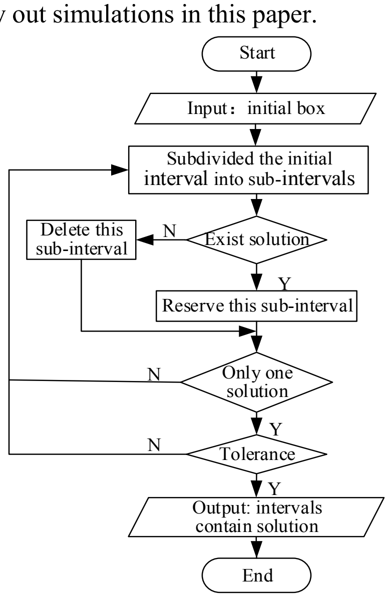

Fig. 2 The process of solving the kinetostatic problem using interval analysis

It is worth noting that the domain of the static equilibrium equation established using the Newton-Euler recursive method is not continuous. Discontinuity points, where the function is undefined, may occur in the equilibrium equation. The most common discontinuity occurs when the cable-driven continuum manipulator is straight. When the endpoint of the sub-interval is close to 0, the inclusion of the solution in the sub-interval cannot be verified. Additionally, depending on the design structure of the cable-driven continuum manipulator, other discontinuity points may exist. Therefore, tiny intervals containing discontinuity points and with a width smaller than the required accuracy must be excluded during function computation.

IV. SIMULATION VERIFICATION

In this section, simulations using MATLAB are carried out to verify the existence of multiple solutions to the kinetostatic problem of continuum manipulators. Specifically, when the external loads and cable driving forces are known, the manipulator may have multiple equilibrium states and its profile cannot be uniquely determined.

C. Simulation setup

The simulation examines both a cable-driven continuum manipulator with a constant cross-section and one with a variable cross-section. In the latter configuration, the cross-sectional area of the central backbone linearly decreases from the manipulator’s base to the end spacer, while keeping the shape and size of the spacer constant. The schematic of the manipulator’s cross-section is shown in Fig. 3 and the parameters of the two manipulators are shown in Table. 1.

In the simulation, the number of the spacers is 3, and the length of the manipulators is 120mm. The initial interval is $[-2\pi/3, 2\pi/3]$, which is the scope of the relative rotation angle of each segment. For the manipulator with constant cross section, the forces of the driving cable are 1.89N and 0N, and the external load is 0.196N. As for the manipulator with variable cross section, the forces of the driving cable are 2.51N and 0N, and the external load is 0.147N. The deflection angle of each segment is noted as α_t ($t=1,2,3$) and the deflection angle of the entire manipulator is noted as α_{sum}.

Table. 1 Structural parameters of the cable-driven continuum manipulators (t=1, ⋯, n)

Parameter	Manipulator with constant cross section	Manipulator with variable cross section
$\overline{a_t O_t}$ (mm)	7.5	7.5
$\overline{b_t O_t}$ (mm)	7.5	7.5
b_{Rt} (mm)	17.1	-0.6×t+18.3
h_R (mm)	2	2
f_t (mm)	40	40
E (Pa)	5.88×10^{7}	5.88×10^{7}
I (kg·m²)	1.14×10^{-11}	$(-0.4\times t+12.2)\times10^{-12}$
m_{ft} (kg)	1.5044×10^{-3}	$(-0.5279\times t+16.0996)\times10^{-4}$
m_{dt} (kg)	0.940×10^{-3}	0.940×10^{-3}
ρ (kg·m⁻³)	1.0997×10^{3}	1.0997×10^{3}

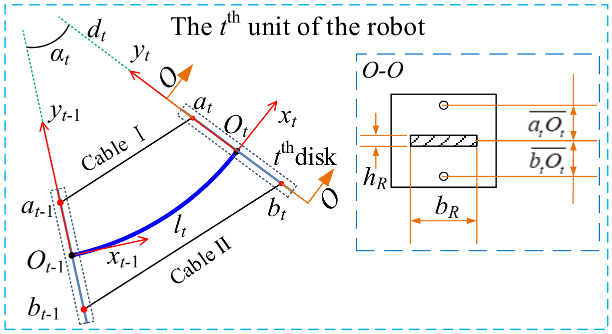

Fig. 3 schematic of the cable-driven continuum manipulator's structural parameters

D. Simulations based on interval analysis method

In this part, simulations on manipulators with both constant and variable cross sections are conducted. The solution of the kinetostatic equations, which is also the deflection angle of each segment of the manipulator, is obtained based on the interval analysis method. Results are shown in Table. 2 and Table. 3, respectively.

Table. 2 Results of the continuum manipulator with constant cross section based on the interval analysis (unit: rad)

Angle	Solution 1	Solution 2	Solution 3
α_1	[-0.09991619568176, -0.09991619568173]	[0.82814267683624, 0.82814267683635]	[1.00336351084447, 1.00336351084456]
α_2	[-0.20988369744885, -0.20988369744881]	[0.91752182127375, 0.91752182127389]	[1.15513939169750, 1.15513939169761]
α_3	[0.33472421331335, 0.33472421331337]	[1.04479830099444, 1.04479830099452]	[1.15074331754074, 1.15074331754078]
α_{Sum}	[0.024924320182740, 0.024924320182830]	[2.790462799104430, 2.790462799104760]	[3.309246220082710, 3.309246220082950]

Table. 3 Results of the continuum manipulator with variable cross section based on the interval analysis (unit: rad)

Angle	Solution 1	Solution 2	Solution 3
α_1	[-0.14005688738858, -0.14005688738846]	[0.59137562024556, 0.59137562024617]	[0.74261573819975, 0.74261573820028]
α_2	[0.34378752862193, 0.34378752862201]	[0.99899441486563, 0.99899441486620]	[1.12985389966658, 1.12985389966700]
α_3	[0.75222788398192, 0.75222788398198]	[1.18422874229864, 1.18422874229895]	[1.24960547233858, 1.24960547233876]
α_{Sum}	[0.95595852521527, 0.95595852521553]	[2.77459877740983, 2.77459877741132]	[3.12207511020491, 3.12207511020604]

E. Simulations based on floating-point optimization algorithm

Table.4 Results the continuum manipulator with constant cross section based on the floating-point optimization algorithm (unit: rad)

Angle	Solution 1	Solution 2	Solution 3
α_1	-0.09991619568174	0.82814267683629	1.00336351084451
α_2	-0.20988369744883	0.91752182127382	1.15513939169755
α_3	0.33472421331336	1.04479830099448	1.15074331754076
α_{Sum}	0.024924320182790	2.790462799104590	3.309246220082820

To facilitate comparison, the Monte Carlo principle [24] is applied to repeatedly perform the calculation based on floating-point optimization algorithm to solve the kinetostatic problem. The initial interval is set to be $[-2\pi/3, 2\pi/3]$. For comparison, the floating-point optimization algorithm is executed for 100 times in this paper. For each execution, the initial iteration point of the optimization algorithm is randomly determined by using the 'rand' function in MATLAB. Simulation results are presented in Table. 4 and Table. 5, respectively.

Table. 5 Results of the continuum manipulator with variable cross section based on the floating-point optimization algorithm (unit: rad)

Angle	Solution 1	Solution 2	Solution 3
α_1	-0.14005688738852	0.59137562024587	0.74261573820003
α_2	0.34378752862197	0.99899441486591	1.12985389966680
α_3	0.75222788398195	1.18422874229879	1.24960547233867
α_{Sum}	0.955958525215400	2.774598777410570	3.122075110205500

Note that the floating-point optimization algorithm is typically executed only once and may not find all solutions to the kinematics. Thus, relying on this algorithm to solve the kinetostatic problem and obtain the profile of the continuum manipulator can be risky.

F. Analysis and discussion

As demonstrated in Tables. 2-5, the results exhibit high precision with an interval width smaller than 1e-11. The solutions obtained by the repeated execution of the floating-point optimization algorithm fall within the intervals determined by the interval analysis method, indicating the effectiveness of this approach.

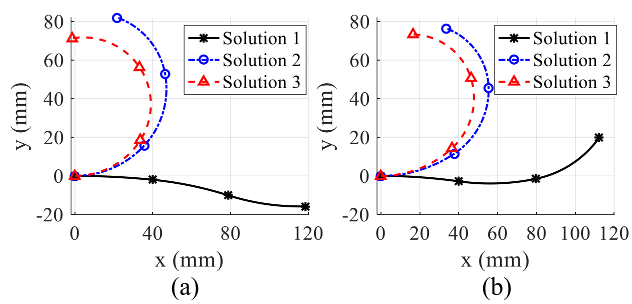

Fig. 4 The profiles corresponding to the solutions ((a) The profiles of the manipulator with constant cross section; (b) The profiles of the manipulator with variable cross section).

Under identical cable tension and external load, both manipulators exhibit three sets of solutions. Figure 4 illustrates the profiles of the cable-driven continuum manipulators corresponding to these multiple solutions, verifying the hypothesis proposed in this paper that the kinetostatic problem of the cable-driven continuum manipulator has multiple solutions, resulting in different profiles when controlling the manipulator. The profiles corresponding to the second and third solutions are similar, indicating that small perturbations may cause sudden profile changes between these two profiles. In contrast, the profile corresponding to the first solution differs significantly from the other two, suggesting that only large external perturbations can alter the manipulator's profile.

It should be noted that the reason that the floating-point optimization algorithm method can obtain multiple solutions in this paper is that it is repeatedly executed intentionally for comparison. Typically, it is executed only once, hence, no more than one solution can be obtained. This underscores the significance of employing the interval analysis method, which can obtain all solutions to the kinetostatic problem. Although this method has the drawback of high computational cost, if the range of the preset interval and the required precision of the solutions are reduced, the computational cost can be significantly reduced. In summary, by using the interval analysis method, the multi-solution problem of the kinetostatics of continuum manipulator is well verified, which has been ignored by previous research.

V.CONCLUSION

This paper proposes a hypothesis that the kinetostatic problem of cable-driven continuum manipulators may have multiple solutions. To investigate this hypothesis, a kinetostatic model based on the Newton-Euler recursion method is employed, and the interval analysis method is applied to solve the nonlinear equations of the kinetostatic model within a preset interval. For comparison, simulations involving repeated execution of commonly used floating-point optimization algorithms at different initial iteration points are conducted. The results demonstrate that there are multiple solutions for the kinetostatic problem of cable-driven continuum manipulators with constant or variable cross-sections, providing preliminary verification of the proposed hypothesis. Furthermore, the results reveal that while the interval analysis method can obtain all solutions to the kinetostatic problem, the commonly used floating-point optimization algorithm method can only obtain one solution, which has been ignored by previous studies.

This paper primarily analyzes and verifies the multiple solutions of the kinetostatic problem of continuum manipulators, filling a gap in the current literature and providing valuable insights for researchers in the field of cable-driven continuum manipulators. However, a drawback of the interval analysis method is its high computational cost, which increases significantly with the number of spacers in the continuum manipulator. In future work, a new approach combining the interval analysis algorithm with modern intelligent optimization algorithms will be considered to improve the computational efficiency of the interval analysis algorithm. Additionally, the application of this method to 3D continuum manipulators with multiple sections will be studied.

REFERENCES

[1] S. Neppalli and B. A. Jones, ‘Design, construction, and analysis of a continuum robot’, in *2007 IEEE/RSJ International Conference on Intelligent Robots and Systems*, 2007, pp. 1503–1507. doi: 10.1109/IROS.2007.4399275.

[2] B. Mazzolai, L. Margheri, M. Cianchetti, P. Dario, and C. Laschi, ‘Soft-robotic arm inspired by the octopus: II. From artificial requirements to innovative technological solutions’, *Bioinspir. Biomim.*, vol. 7, no. 2, p. 025005, May 2012, doi: 10.1088/1748-3182/7/2/025005.

[3] D. Axinte *et al.*, ‘MiRoR—Miniaturized Robotic Systems for Holistic *In-Situ* Repair and Maintenance Works in Restrained and Hazardous Environments’, *IEEE/ASME Trans. Mechatron.*, vol. 23, no. 2, Art. no. 2, Apr. 2018, doi: 10.1109/TMECH.2018.2800285.

[4] G. Z. Meng, L. Y. Sun, P. Peng, X. C. Meng, H. M. Wang, and J. W. Zhang, ‘Jacobian Matrix of a Novel Continuum Robot for Search and Rescue’, *Applied Mechanics and Materials*, vol. 303–306, pp. 1695–1701, 2013, doi: 10.4028/www.scientific.net/AMM.303-306.1695.

[5] Z. Wu, C. Zhu, Y. Ding, Y. Wang, B. Xu, and K. Xu, ‘A robotic surgical tool with continuum wrist, kinematically optimized curved stem, and collision avoidance kinematics for single port procedure’, *Mechanism and Machine Theory*, vol. 173, p. 104863, Jul. 2022, doi: 10.1016/j.mechmachtheory.2022.104863.

[6] Y. Dai, Z. Li, X. Chen, X. Wang, and H. Yuan, ‘A Novel Space Robot with Triple Cable-Driven Continuum Arms for Space Grasping’, *Micromachines*, vol. 14, no. 2, Art. no. 2, Feb. 2023, doi: 10.3390/mi14020416.

[7] R. Buckingham and A. Graham, ‘Nuclear snake-arm robots’, *Industrial Robot: An International Journal*, vol. 39, no. 1, pp. 6–11, Jan. 2012, doi: 10.1108/01439911211192448.

[8] X. Dong, D. Palmer, D. Axinte, and J. Kell, ‘In-situ repair/maintenance with a continuum robotic machine tool in confined space’, *Journal of Manufacturing Processes*, vol. 38, pp. 313–318, Feb. 2019, doi: 10.1016/j.jmapro.2019.01.024.

[9] C. Yang *et al.*, ‘Geometric constraint-based modeling and analysis of a novel continuum robot with Shape Memory Alloy initiated variable stiffness’, *The International Journal of Robotics Research*, p. 027836492091392, Apr. 2020, doi: 10.1177/0278364920913929.

[10] X. Dong *et al.*, ‘Development of a slender continuum robotic system for on-wing inspection/repair of gas turbine engines’, *Robotics and Computer-Integrated Manufacturing*, vol. 44, pp. 218–229, Apr. 2017, doi: 10.1016/j.rcim.2016.09.004.

[11] K. Xu and N. Simaan, ‘An Investigation of the Intrinsic Force Sensing Capabilities of Continuum Robots’, *IEEE Trans. Robot.*, vol. 24, no. 3, pp. 576–587, Jun. 2008, doi: 10.1109/TRO.2008.924266.

[12] H. Yuan and Z. Li, ‘Workspace analysis of cable-driven continuum manipulators based on static model’, *Robotics and Computer-Integrated Manufacturing*, vol. 49, pp. 240–252, Feb. 2018, doi: 10.1016/j.rcim.2017.07.002.

[13] H. Yuan, W. Zhang, Y. Dai, and W. Xu, ‘Analytical and numerical methods for the stiffness modeling of cable-Driven serpentine manipulators’, *Mechanism and Machine Theory*, vol. 156, p. 104179, Feb. 2021, doi: 10.1016/j.mechmachtheory.2020.104179.

[14] R. E. Moore, ‘Interval analysis’, 1959. Accessed: Feb. 15, 2023. [Online]. Available: doi: 10.1090/psapm/010/0116636

[15] A. M. Andrew, ‘Applied Interval Analysis: With Examples in Parameter and State Estimation, Robust Control and Robotics’, *Kybernetes*, vol. 31, no. 5, Jan. 2002, doi: 10.1108/k.2002.06731eae.002.

[16] A. Berti, J.-P. Merlet, and M. Carricato, ‘Solving the direct geometrico-static problem of underconstrained cable-driven parallel robots by interval analysis’, *The International Journal of Robotics Research*, vol. 35, no. 6, pp. 723–739, May 2016, doi: 10.1177/0278364915595277.

[17] D. C. Rucker and R. J. W. III, ‘Statics and Dynamics of Continuum Robots With General Tendon Routing and External Loading’, *IEEE Transactions on Robotics*, vol. 27, no. 6, pp. 1033–1044, Dec. 2011, doi: 10.1109/TRO.2011.2160469.

[18] K. Xu and N. Simaan, ‘Analytic Formulation for Kinematics, Statics, and Shape Restoration of Multibackbone Continuum Robots Via Elliptic Integrals’, *Journal of Mechanisms and Robotics*, vol. 2, no. 1, p. 011006, Feb. 2010, doi: 10.1115/1.4000519.

[19] R. E. Moore, R. B. Kearfott, and M. J. Cloud, *Introduction to Interval Analysis*. Society for Industrial and Applied Mathematics, 2009. doi: 10.1137/1.9780898717716.

[20] S. Iqbal, S. Mohammed, and Y. Amirat, ‘A guaranteed approach for kinematic analysis of continuum robot based catheter’, in *2009 IEEE International Conference on Robotics and Biomimetics (ROBIO)*, Guilin, China: IEEE, Dec. 2009, pp. 1573–1578. doi: 10.1109/ROBIO.2009.5420395.

[21] F. Hisch, A. Giusti, and M. Althoff, ‘Robust Control of Continuum Robots using Interval Arithmetic’, *IFAC-PapersOnLine*, vol. 50, no. 1, pp. 5660–5665, Jul. 2017, doi: 10.1016/j.ifacol.2017.08.1115.

[22] R. E. Moore, "Methods and applications of interval analysis," in SIAM Studies in Applied Mathematics, Society for Industrial and Applied Mathematics, Philadelphia, 1979.

[23] H. Wang, D. Cao, and S. Li, ‘An interval entropy method for equality constrained multiobjective optimization problems’, *Numer. Analys. Appl.*, vol. 1, no. 1, pp. 25–33, Jan. 2008, doi: 10.1134/S1995423908010035.

[24] R. Barea, E. Lopez, L. M. Bergasa, S. Alvarez, and M. Ocana, ‘Detection Model in Collaborative Multi-Robot Monte Carlo Localization.’, in *IEEE Workshop on Distributed Intelligent Systems: Collective Intelligence and Its Applications (DIS’06)*, Jun. 2006, pp. 49–54. doi: 10.1109/DIS.2006.24.